



Stratospheric water vapor and ozone response to different QBO disruption events in 2016 and 2020

Mohamadou A. Diallo¹, Felix Ploeger^{1, 2}, Michaela I. Hegglin^{1, 2, 3}, Manfred Ern¹, Jens-Uwe Grooß¹, Sergey Khaykin⁴, and Martin Riese^{1, 2}

¹Institute of Energy and Climate Research, Stratosphere (IEK-7), Forschungszentrum Jülich, 52 425 Jülich, Germany.

²Institute for Atmospheric and Environmental Research, University of Wuppertal, Wuppertal, Germany.

³Department of Meteorology, University of Reading, Reading, UK.

⁴Laboratoire Atmosphères, Milieux, Observations Spatiales, UMR CNRS 8190, IPSL, Sorbonne Univ./UVSQ, Guyancourt, France.

Correspondence: Mohamadou A. Diallo (m.diallo@fz-juelich.de)

Abstract. The Quasi-Biennial Oscillation (QBO) is a major mode of climate variability with periodically descending westerly and easterly winds in the tropical stratosphere, modulating transport and distributions of key greenhouse gases such as water vapor and ozone. In 2016 and 2020, anomalous QBO easterlies disrupted the QBO's 28-month period previously observed. Here, we quantify the impact of these two QBO disruption events on the Brewer–Dobson circulation, water vapour and ozone using the ERA5 reanalysis and satellite observations, respectively. Both lower stratospheric trace gases decrease globally during the 2015–2016 QBO disruption event, while they only weakly decrease during the 2019–2020 QBO disruption event. These dissimilarities in the circulation anomalous response to the QBO disruption events result from differences in the tropical upwelling caused by anomalous planetary and gravity wave forcing in the lower stratosphere near the equatorward flanks of the subtropical jet. The differences in the response of lower stratospheric water vapor to the 2015–2016 and 2019–2020 QBO disruption events are due to the cold–point temperature differences induced by the Australian wildfire, which moistened the lower stratosphere, therefore, hiding the 2019–2020 QBO disruption impact. Our results highlight the need for a better understanding of the causes of QBO disruption events, their interplay with other climate variability modes, and their impacts on water vapor and ozone in the face of a changing climate.

15 1 Introduction

The upper troposphere and lower stratosphere (UTLS) is a key region of the Earth climate system because of its large sensitivity to radiative forcing of greenhouse gases, such as water vapor (H₂O) and ozone (O₃) (Gettelman et al., 2011; Dessler et al., 2013; Nowack et al., 2015). Any changes in the composition of these radiatively active trace gases in the UTLS region induced by the stratospheric Brewer–Dobson circulation (BDC) and its modulation by the modes of climate variability lead to large impact



20 on surface climate (e.g., Forster and Shine, 2002, 1999; Solomon et al., 2010; Riese et al., 2012; Butchart, 2014; Diallo et al.,
2017, 2018, 2019, 2021). Ozone is mainly produced in the middle stratosphere and is a good proxy of the tropical upwelling.
In addition, ozone variability in the tropical lower stratosphere is affected by variability in tropical upwelling of the BDC
(Randel et al., 2007; Abalos et al., 2013; Stolarski et al., 2014). The ozone transport and lifetime in the UTLS region are both
modulated by the seasonality in the BDC and the natural modes of climate variability, including the Quasi-Biennial Oscillation
25 (QBO) (Randel and Thompson, 2011; Diallo et al., 2018). Lower stratospheric water vapor and its multi-timescale variations
ranging from day to decades are mainly controlled by changes in the tropical cold point temperatures and its modulations by
the natural modes of climate variability, including the QBO (Holton and Gettelman, 2001; Hu et al., 2016; Diallo et al., 2018;
Tao et al., 2019; Randel and Park, 2019). Therefore, the amount of water vapor in the UTLS region is directly linked to the
dehydration in the air parcels crossing through the coldest temperatures in the tropical tropopause layer (e.g., between 14 and
30 19 km; Fueglistaler et al., 2009).

Considered as a dominant mode of variability of the equatorial stratosphere, the QBO globally impacts the transport and
distributions of stratospheric water vapor and ozone. Mostly driven by gravity waves and equatorially trapped waves, the QBO
is a quasi-periodic oscillation between tropical westerly and easterly zonal wind shears (Baldwin et al., 2001; Ern et al., 2014).
Both QBO phases modulate the vertical and meridional components of the BDC and affect temperature structure, therefore,
35 impacting the water vapor and ozone composition and radiative feedback in the UTLS region (Plumb and Bell, 1982; Niwano
et al., 2003; Diallo et al., 2018).

The quasi-periodic QBO cycle of about 28-month period, which alternates between westerly and easterly zonal wind shears,
was subject to two disruptions in the past five years. In January 2016 and 2020, the anomalous QBO westerlies in the tropical
lower stratosphere were unexpectedly interrupted by anomalous QBO easterlies caused by planetary waves propagating from
40 the mid-latitudes toward the equatorial region combined with equatorial convective gravity waves (Osprey et al., 2016; Coy
et al., 2017; Kang et al., 2020; Kang and Chun, 2021). There is not yet a clear understanding of how these QBO disruptions are
linked to anomalously warm or cold sea surface temperatures (Taguchi, 2010; Schirber, 2015; Dunkerton, 2016; Christiansen
et al., 2016; Barton and McCormack, 2017), volcanic aerosols (Kroll et al., 2020; DallaSanta et al., 2021), wildfire smoke
(Khaykin et al., 2020; Yu et al., 2021; Peterson et al., 2021) and climate changes (Anstey et al., 2021b). However, recent study
45 based on climate model simulations from phase six of the Coupled Model Intercomparison Project (CMIP6) predicts increased
disruption frequencies to the quasi-regular QBO cycle in a changing climate (Osprey et al., 2016; Anstey et al., 2021b).
Previous studies also suggest that the QBO amplitude in the tropical stratosphere is decreasing in the lower stratosphere due
to the climate change-induced strengthening of tropical upwelling (Saravanan, 1990; Kawatani et al., 2011; Kawatani and
Hamilton, 2013). Thus, in the context of a changing climate, the predictable QBO signal associated with the quasi-regular
50 phase progression and amplitude as well as its potential impacts on UTLS composition faces an uncertain future. Therefore, it
is of particular importance to quantify and better understand the different impact of the QBO disruption events on UTLS water
vapor and ozone, which have the potential to globally affect the radiative forcing of the Earth's climate system (Forster and
Shine, 1999; Butchart and Scaife, 2001; Solomon et al., 2010; Riese et al., 2012).



Here, we quantify the similarity and differences in the strength and depth between the 2015–2016 and 2019–2020 disrupted
55 QBO impacts on lower stratospheric water vapor and ozone from satellite observations. Also, we analyse the main drivers of
the differences in anomalous circulation and UTLS composition changes. Section 2 describes the satellite observational data
sets and the multivariate hybrid regression model used for the quantification. Section 3 describes the anomalous BDC and
UTLS composition changes following the 2016 and 2020 QBO disruption events. Section 4 discusses the results of a well-
established multivariate hybrid regression analysis to provide evidence for the impact of the QBO disruption events on lower
60 stratospheric water vapor and ozone. Finally, we discuss the main reasons of the anomalous BDC and UTLS composition
differences between the 2015–2016 and 2019–2020 disrupted QBO impacts in relationship to planetary and gravity wave
dissipation likely caused by the anomalous surface conditions associated with the strong El Niño Southern Oscillation (ENSO)
in 2015–2016, the strong Indian Ocean Dipole (IOD) in 2019–2020. We further discuss the differences between 2016 and 2020
in view of the particularly warmer stratosphere linked to Australian wildfire smoke in 2020.

65 2 Data and methodology

To quantify the QBO impact, we used the monthly mean zonal mean ozone and water vapor mixing ratios from the Aura
Microwave Limb Sounder (MLS) satellite observations covering the 2005–2020 period (Livesey et al., 2017). The version 4.4
MLS data set used here has a vertical resolution of 2.5–3 km ranging from 8 to 35 km and 60°S/N with a high precision and
lower systematic uncertainty (Santee et al., 2017). Previous findings show that MLS zonal monthly mean H₂O mixing ratios
70 show very good agreement with the multi-instrument mean (Hegglin et al., 2013, 2021).

In addition to the MLS observation data sets, we also utilize the temperature (T) and zonal mean wind (U) from the ERA5
reanalysis of the European Centre for Medium-Range Weather Forecasts (ECMWF) (Hersbach et al., 2020). We have also
calculated the residual circulation vertical velocity ($\overline{w^*}$) using the Transformed Eulerian Mean (TEM; Andrews et al. (1987))
and decomposed the wave drag into planetary (PWD) and gravity (GWD) wave drag contributions to the circulation anomalies
75 (Ern et al., 2014, 2021). Note that we are using the ERA5 reanalysis data on the original 137 model levels for calculating the
TEM budget, but not the coarse conventional pressure-level data, which can cause large uncertainties in the equatorial waves
and zonal wind in the tropical stratosphere (Fujiwara et al., 2012; Kim and Chun, 2015; Kawatani et al., 2016). For more details
about the ERA5 TEM calculations and wave decomposition please see Diallo et al. (2021).

We disentangle the QBO impact on these monthly mean zonal mean stratospheric water vapor and ozone mixing ratios from
80 the other sources of natural climate variability using a multivariate hybrid regression model for the 2005–2020 period (Eq. 1).
To highlight the two QBO disruptions, figures only show the 2013–2020 period. The established multivariate hybrid regression
method is appropriate to separate the relative influences of the considered modes of climate variability, including the QBO, on
stratospheric water vapor and ozone. Additional details about the multivariate hybrid regression model and its applications can
be found in Diallo et al. (2018). Our multivariate hybrid regression model decomposes the given monthly zonal mean variable,
85 Var_i , into a long-term linear trend, seasonal cycle, modes of climate variability and a residual (ϵ). For a given variable Var_i
(herein H₂O, O₃, $\overline{w^*}$, T, PWD and GWD), the multivariate hybrid regression model yields



$$\text{Var}_i(t_{\text{month}}, y_{\text{lat}}, z_{\text{alt}}) = \text{Trend}(t_{\text{month}}, y_{\text{lat}}, z_{\text{alt}}) + \text{SeasCyc}(t_{\text{month}}, y_{\text{lat}}, z_{\text{alt}}) + \sum_{n=1}^5 b_n(y_{\text{lat}}, z_{\text{alt}}) \cdot \text{Proxy}_n(t_{\text{month}} - \tau_n(y_{\text{lat}}, z_{\text{alt}})) + \varepsilon(t_{\text{month}}, y_{\text{lat}}, z_{\text{alt}}), \quad (1)$$

where Proxy_n represents the different climate indexes used here. Proxy_1 is a normalized QBO index (QBOi) from the tropical ERA5 zonally averaged tropical zonal mean winds with full vertical levels then deseasonalised and normalized by the standard deviation to build the QBOi (Hersbach et al., 2020). Proxy_2 is the normalized Multivariate ENSO Index (MEI; Wolter and Timlin, 2011), Proxy_3 is the Indian Ocean Dipole (IOD, Saji et al., 1999), Proxy_4 is the Madden-Julian Oscillation (MJO, Son et al., 2017), and Proxy_5 is the AOD from satellite data (Thomason et al., 2018). $\text{Trend}(t_{\text{month}}, y_{\text{lat}}, z_{\text{alt}})$ is a linear trend. $\text{SeasCyc}(t_{\text{month}}, y_{\text{lat}}, z_{\text{alt}})$ is the annual cycle. The coefficients are the amplitude b_n and the lag $\tau_n(y_{\text{lat}}, z_{\text{alt}})$ associated with the QBO, ENSO, IOD, MJO and AOD respectively. The solar forcing is neglected because our data set is relatively short. Finally, we estimate the uncertainty in the multivariate hybrid regression model using a Student's t test technique (von Storch and Zwiers, 1999; Friston et al., 2007).

3 Characterisation of the 2016 and 2020 anomalous circulations

In February 2016 and January 2020 unexpected tropical QBO easterlies (negative QBOi) developed in the center of the tropical QBO westerlies, thereby breaking the quasi-regular QBO cycle of alternating easterly and westerly phases (Fig. 1a) (Osprey et al., 2016; Newman et al., 2016; Anstey et al., 2021a). Both QBO disruption events have been associated with a combination of extratropical Rossby waves, equatorial planetary waves (Kelvin, Rossby, mixed Rossby–gravity, and inertia–gravity), and small-scale convective gravity waves, propagating into the deep tropics and depositing their negative momentum forcing (Osprey et al., 2016; Newman et al., 2016; Kang et al., 2020; Kang and Chun, 2021). Both QBO disruption events are primarily triggered by mid-latitude Rossby waves propagating from the northern hemisphere in 2015–2016 and from the southern hemisphere in 2019–2020 into the deep tropics. In 2015–2016, the equatorial planetary wave forcing may have preconditioned mid-latitude Rossby waves to break easily at the equator (e.g. Lin et al. (2019)), while in 2019–2020, the equatorial planetary and small-scale convective gravity waves propagating into the UTLS predominantly contributed to the disruption (Kang et al., 2020; Kang and Chun, 2021). Note that the potential processes and mechanisms triggering the QBO disruption are still under debate. Recent findings from Match and Fueglistaler (2021) using a 1D theoretical model of the QBO from Plumb and Bell (1982) pointed out the key role of the upwelling and wave dissipation. For more details about the triggering please see these studies (Schirber, 2015; Dunkerton, 2016; Christiansen et al., 2016; Coy et al., 2017; Barton and McCormack, 2017; Hitchcock et al., 2018; Watanabe et al., 2018; Renaud et al., 2019; Match and Fueglistaler, 2021). Although similar in many respects, including the causes of the sudden development of tropical QBO easterlies in the center of tropical QBO westerlies, the two disruptions also exhibit differences, particularly in the structure (strength and depth) of the impacts and the level at which it started. Here, we mainly focus on the impact of the QBO disruption events on the lower stratospheric BDC and trace gases, including water vapour and ozone.

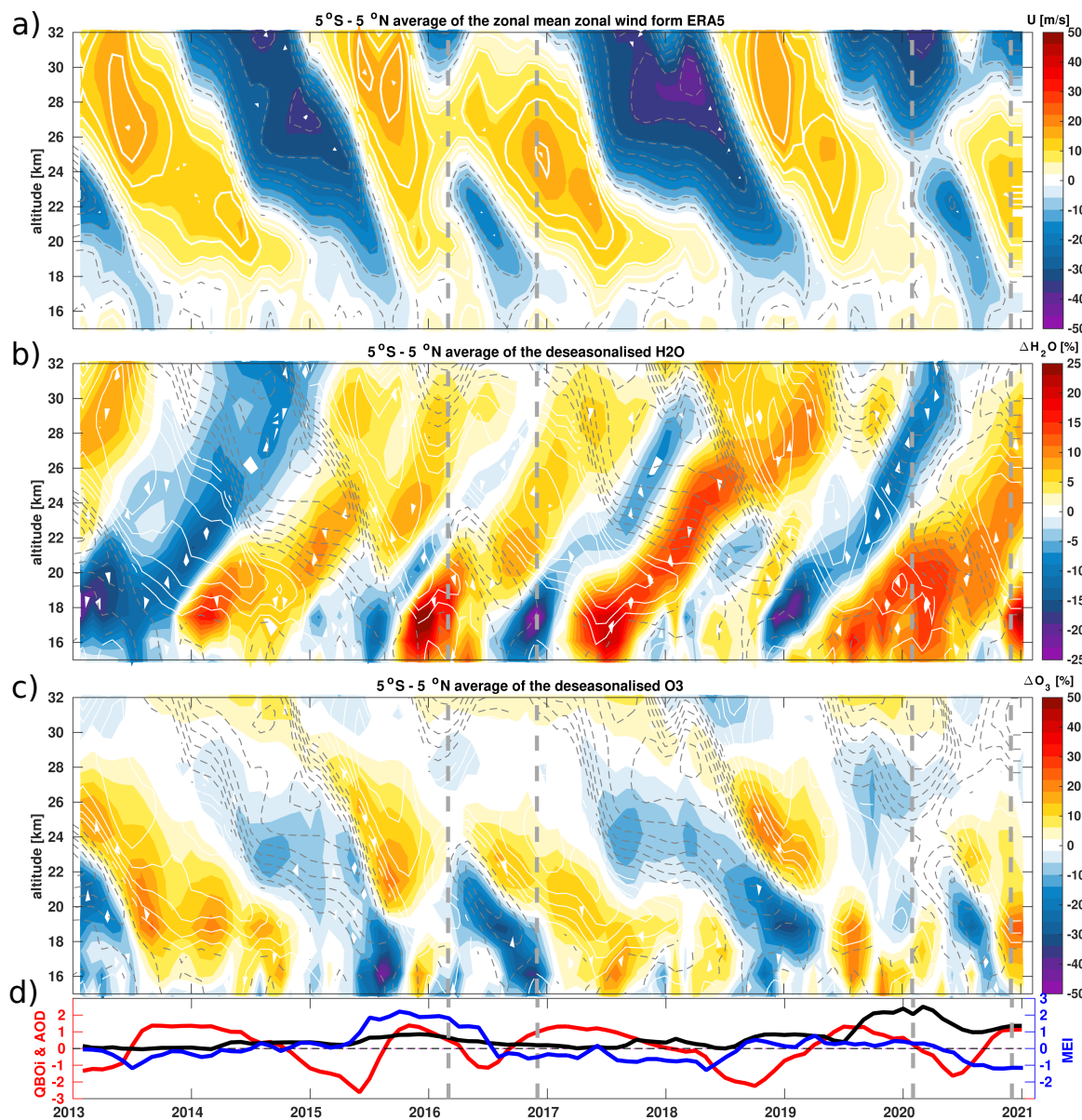


Figure 1. Tropical average of the zonal mean zonal wind (U) from ERA5 (a) and deseasonalized stratospheric H_2O and O_3 time series from MLS satellite observations for the 2013–2020 period in percent change from long-term monthly means as a function of time and altitude. Shown are (a) Zonal mean zonal wind U , (b) Deseasonalized monthly mean H_2O anomalies, (c) Deseasonalized monthly mean O_3 anomalies. Vertical grey dashed lines indicate the QBO disruption onset and offset years. The lowermost panel (d) shows the QBO index at 50 hPa in red, the MEI index in blue and the AOD index in black. Monthly averaged zonal mean zonal wind component, u ($m s^{-1}$), from ERA5, is overlaid as solid white (westerly wind) and dashed gray (easterly wind) contour lines.



The similarities as well as the differences between the two disruption events are also visible in the inter-annual variability of the tropical lower stratospheric zonal mean zonal wind (a), H₂O (b) and O₃ (c) anomalies as a percentage change relative to the monthly mean mixing ratio during the 2013–2020 period (Fig. 1a–c). Both QBO disruption events are expected to impact the tropical upwelling of the BDC through the two way interactions between the mean–flow and wave propagation associated with the QBO phases (Plumb, 1977; Lindzen, 1971; Holton, 1979; Dunkerton, 1980; Plumb and Bell, 1982; Grimshaw, 1984; Match and Fueglistaler, 2021) as well as through its control of the tropical cold point temperatures (Kim and Son, 2012; Kim and Chun, 2015). This impact of the 2015–2016 and 2019–2020 QBO disruption events on the transport and distribution of lower stratospheric H₂O and O₃ mixing ratios is the most effective when the signal reaches the tropical cold point temperature altitude (~17 km) e.g. from June to December in 2016 and from June to August in 2020 (Fig. 1) (Tweedy et al., 2017; Diallo et al., 2018). The zonal mean zonal wind shows that the westerly jet at 30 hPa is stronger and deeper during the 2015–2016 QBO disruption than the 2019–2020 QBO disruption (Fig. 1a and Fig. S1a–b in the supplement). The 2019–2020 QBO disruption shows a clear cut of the westerlies into two parts while the 2015–2016 QBO disruption shifts the westerlies upward (Fig. 1a). As soon as the downward propagation of tropical QBO easterlies reaches the tropical cold point temperature (~17 km) from June to December 2016, the H₂O mixing ratios decrease i.e. turning from positive to negative anomalies. As reported by Diallo et al. (2018), the alignment of the strong El Niño event with westerly QBO in early boreal winter of 2015–2016 (September 2015–March 2016) substantially increased H₂O mixing ratios and decreased O₃ mixing ratios up to about 20 % in the tropical lower stratosphere between the tropopause and the altitude of 25 km (Fig. 1b, c). Then, the sudden occurrence of the QBO disruption decreased the lower stratospheric H₂O and O₃ mixing ratios from late spring to early following winter up to about 20 %.

Conversely during the 2019–2020 QBO disruption, Figure 1b, c show clear differences in the tropical lower stratospheric trace gas anomalies, particularly in the strength and depth of H₂O and O₃ anomalies, consistent with the structural zonal mean zonal wind changes (Fig. S1a, b). The tropical lower stratospheric O₃ anomalies are purely responding to the enhanced tropical upwelling of the BDC caused in 2016 by a combination of a strong El Niño event, negative IOD event and the QBO disruption in 2015–2016, and in 2020 by a combination of a weak La Niña, strong positive IOD event and the QBO disruption in 2019–2020 (e.g., easterly winds at 100–40 hPa). Tropical lower stratospheric O₃ anomaly is a good proxy of the tropical upwelling of the BDC as its concentration is modulated by the advection of tropospheric air generally poor in O₃ into the stratosphere (Randel et al., 2006; Abalos et al., 2013; Stolarski et al., 2014; Weber et al., 2011; Iglesias-Suarez et al., 2021). The small decrease in the tropical lower stratospheric O₃ anomalies up to about 10 % in 2020 compare to about 20% in 2016 between the altitude of 16 km and 25 km suggests a stronger tropical upwelling and its modulations in 2016 than in 2020 (Fig. 1c and Fig. S3a in the supplement).

The tropical lower stratospheric H₂O variability (tape recorder) is more challenging to interpret because of its regulation by the variability in the tropical cold point temperatures (Holton and Gettelman, 2001; Hu et al., 2016; Randel and Park, 2019). The negative tropical lower stratospheric H₂O anomalies induced by the interplay of different modes of natural climate variability, including the QBO, are weaker in 2020 than in 2016 (Fig. 1b and Fig. S2a, b in the supplement). The tropical lower stratospheric H₂O anomalies averaged between the altitude of 16 km and 20 km are up to about 20 % more negative in



2016 than in 2020 (Fig. S3a in the supplement). Particularly, the 2020 tape recorder shows large positive H₂O anomalies even after the QBO disruption that are of opposite sign to the 2016 H₂O anomalies (Fig. 1b). This complexity in H₂O inter-annual variability lies in its dependency on the interplay of different modes of natural climate variability, including the QBO phases (Diallo et al., 2018; Brinkop et al., 2016; Tian et al., 2019; Liess and Geller, 2012), seasons (early or late in the winter) and location (western, central or eastern Pacific, where the ENSO and IOD maximum occurs (Garfinkel et al., 2013; Smith et al., 2021)). Therefore, to elucidate the effect of both QBO disruption events on the lower stratospheric H₂O and O₃ anomalies, we performed regression analysis both without and with explicitly including QBO signals to isolate the QBO impact on these trace gases. The difference between the residual (ϵ in Eq. 1) with and without explicit inclusion of the QBO signals gives the QBO-induced impact on stratospheric H₂O and O₃ anomalies. This approach of differencing the residuals is similar to direct calculations, projecting the regression fits onto the QBO basis functions, i.e., the QBO predictor timeseries (see supplement Figs. 2 and 4 in (Diallo et al., 2017)). In addition, this differencing approach avoids the need to reconstruct the time series after the regression analysis.

4 Drivers detection and attribution of the anomalous circulations

4.1 Impact of QBO disruptions on UTLS composition

Figures 2a, b show time series of the QBO-induced inter-annual variability in tropical lower stratospheric H₂O and O₃ anomalies estimated from the difference between the residual (ϵ in Eq. 1) without and with explicit inclusion of the QBO proxy for the 2013–2020 period. A footprint of both QBO disruption events is clearly visible in lower stratospheric H₂O and O₃ anomalies with a shift from positive anomalies related to the westerly winds (positive QBO_i) to negative anomalies related to the easterly winds (negative QBO_i). The QBO disruption-induced O₃ anomalies are sudden and clearly follow the monthly mean zonal mean wind changes. The QBO disruption-induced H₂O anomalies are roughly in phase with the zonal wind anomalies with a delay of about 3–6 months because of the H₂O tropospheric origin as well as its dependency on the tropical cold point temperature anomaly.

Beside the good agreement in the structure of both trace gas changes, there are clear differences in the strength and depth of both lower stratospheric H₂O and O₃ responses to the QBO disruptions between the 2016 and the 2020 events and, particularly large for the H₂O response. These differences in the impact of the QBO disruption events are consistent with the observed lower stratospheric H₂O and O₃ anomalies (Fig. 1, Fig. S2 and S3). During 2016, the QBO shift from westerlies to easterlies at 40 hPa in the tropical lower stratosphere induces substantial negative H₂O and O₃ anomalies up to about 20 % between the altitude of 16 km and 25 km from the early boreal spring to the next boreal winter (Fig. 2). This decrease in H₂O and O₃ mixing ratios is consistent with upward transport of young and dehydrated air poor in H₂O and O₃ into the lower stratosphere between the altitude of 16 km and 25 km. As expected, the sudden occurrence of the QBO disruption events caused anomalously cold point temperatures and enhanced tropical upwelling in 2016 and in 2020, consistent with the decrease in H₂O and O₃ mixing ratios induced by the QBO easterly (Fig. 2). However, besides the similarities in the structural changes, the negative H₂O and O₃ anomalies induced by the QBO disruption are smaller and shallower in 2020 than in 2016. While the differences in



the O_3 anomalies induced by the QBO disruption events are small between the year 2016 and year 2020, the differences in the disrupted QBO impact on O_3 mixing ratios are particularly large between the year 2016 and year 2020 (Fig. 2a and Fig. S3b in the supplement). The differences in the magnitude of negative O_3 anomalies suggest a slightly weaker modulation of the anomalous tropical upwelling of the BDC by the secondary circulation in 2020 than in 2016, consistent with the differences
190 in the strength and depth of the residual vertical velocity and wave forcing anomalies discussed in Sect. 4.2. The differences in the strength and depth of the H_2O response to the QBO disruption events suggest that the tropical cold point temperature is substantially different between the year 2016 and year 2020. In addition, we note that the early QBO westerly followed by the shift to QBO easterly is not the main cause of the large increase in the 2020 lower stratospheric H_2O anomalies. In the following, we assess the potential impact of the unusually strong Australian wildfire smoke on the lower stratospheric H_2O
195 anomalies in 2020 through its impact on the stratospheric temperature anomaly (Khaykin et al., 2020; Yu et al., 2021; Peterson et al., 2021).

Figures 3a–d show the zonal mean impact of the QBO disruption events on lower stratospheric H_2O and O_3 anomalies. Figure 3e shows the impact of 2020 Australian wildfire AOD on lower stratospheric H_2O anomalies. The lower stratospheric H_2O anomalies are averaged from July to December for 2016 and from July to September for 2020 respectively. We chose
200 different averaging periods for 2016 (July–to–December) and 2020 (July–August–September) to have similar zonal mean structure of the H_2O and O_3 anomalies response to QBO disruptions, although their depth and strength are different from each other.

In 2016, the shift to QBO easterly phase in the tropics significantly dehydrates the global lower stratosphere up to about 20 % below the altitude of 20 km (Fig. 3a and Fig. S2a) (Diallo et al., 2018; Tweedy et al., 2017). This decrease in H_2O mixing ratios
205 is due to the enhanced tropical upwelling of the BDC, its modulation by the secondary circulation and the related decrease of tropical cold point temperature as discussed later in Sect. 4.2 (Diallo et al., 2018; Jensen et al., 1996; Hartmann et al., 2001; Geller et al., 2002; Schoeberl and Dessler, 2011). Because of the hemispheric asymmetry of the BDC strength, which is driven by planetary wave activity (e.g. Holton and Gettelman, 2001) and eddy mixing (e.g. Haynes and Shuckburgh, 2000), the rising dehydrated air from the tropics moves toward middle and high latitudes of both hemispheres, but stronger in winter
210 hemisphere. The positive H_2O anomalies above the altitude of 20 km are related to the effect of the preceding QBO westerly phase on tropical UTLS temperatures and the upward propagating tape-recorder signal. The changes in H_2O anomalies are consistent with the observed negative tropical O_3 anomalies below the altitude of 20 km induced by the QBO easterly phase (Fig. 3a, c and Fig. S2a, c in the supplement). These changes indicate an enhanced tropical upwelling of the BDC and its modulation by the QBO easterly phase in the lower stratosphere between the altitude of 16 km and 20 km (Fig. S4 in the
215 supplement). Above the altitude of 20 km, the positive tropical O_3 anomalies are associated with the QBO westerly phase (Fig. 3c and Fig. S2c in the supplement). Also note the large variability in extratropical O_3 anomalies related to the QBO influence on the extratropical circulation (Holton and Tan, 1980; Damadeo et al., 2014; Ray et al., 2020), stratospheric major warmings, and chemical processes (WMO, 2018).

In 2020, the QBO disruption–induced changes in tropical lower stratospheric H_2O and O_3 anomalies exhibit similar struc-
220 ture to the effect of the 2015–2016 QBO disruption event. Note that we use different averaging periods for 2016 (July–to–

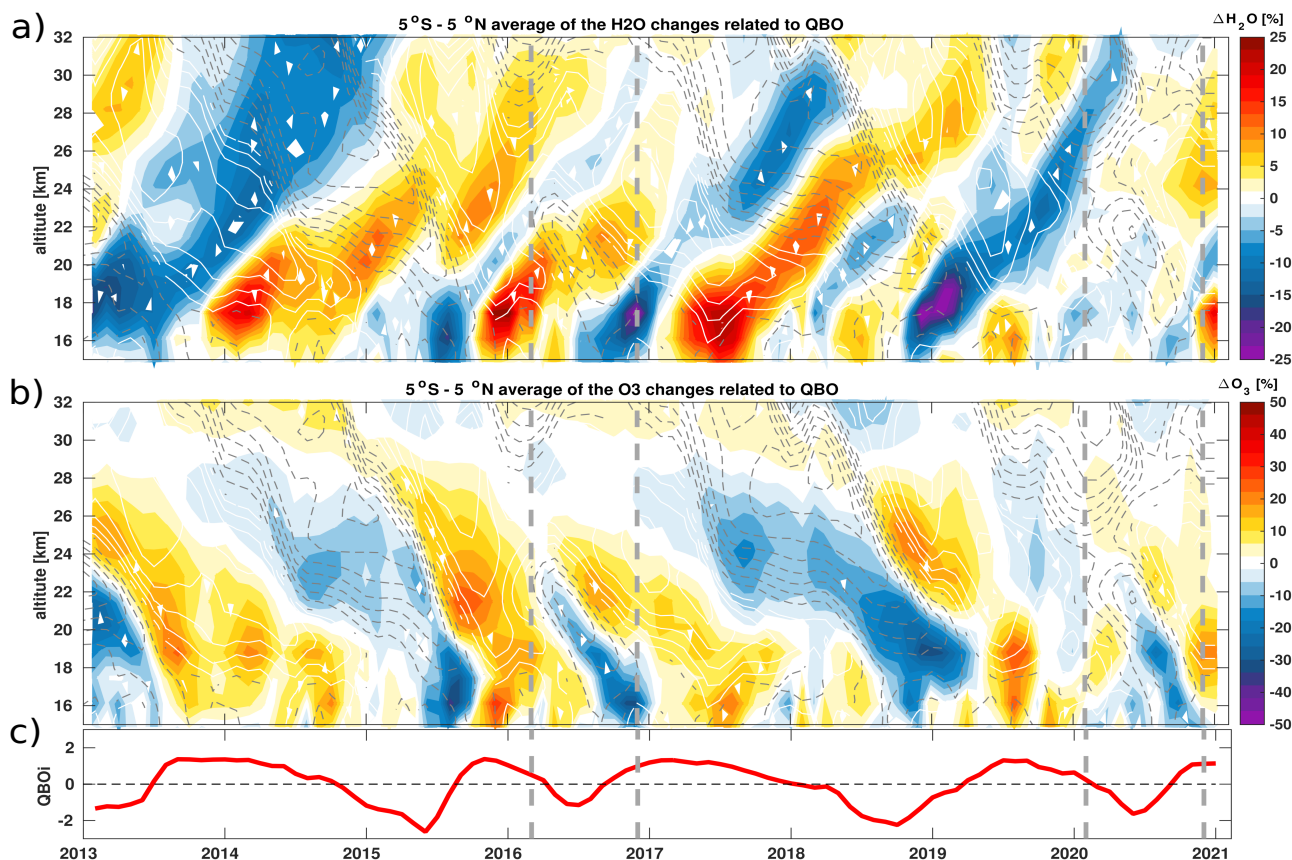


Figure 2. Tropical average of the QBO impact on the stratospheric H₂O (a) and O₃ (b) anomalies from the MLS satellite observations for the 2013–2020 period in percent change relative to monthly mean mixing ratios as a function of time and altitude. Shown QBO impact on the stratospheric trace gases is derived from the multiple regression fit as the difference between the residual (ϵ in Eq. 1) without and with explicit inclusion of the QBO signal. The lower panel below indicates the QBO index at 50 hPa in red. Vertical grey dashed lines indicate the QBO disruption onset and offset years. Monthly averaged zonal mean zonal wind component, u (m s^{-1}), from ERA5, is overlaid as solid white contours (westerly) and dashed gray contours (easterly) lines.

December) and 2020 (JAS) to highlight the structural similarities in the QBO impact. Both trace gases show negative anomalies in the tropics, corroborating the enhanced tropical upwelling of the BDC induced by the QBO shift from westerly winds to easterly winds in the tropics (Fig. 3b). However, there are also differences in both lower stratospheric H₂O and O₃ responses to the shift from the tropical QBO westerly phase to the tropical QBO easterly phase between July–to–December 2016 and 2020 (JAS). Note that the differences in the H₂O response to the QBO disruption events between the year 2016 and the year 2020 are particularly large. Conversely to the globally dehydrated lower stratosphere in 2016, the sudden development of

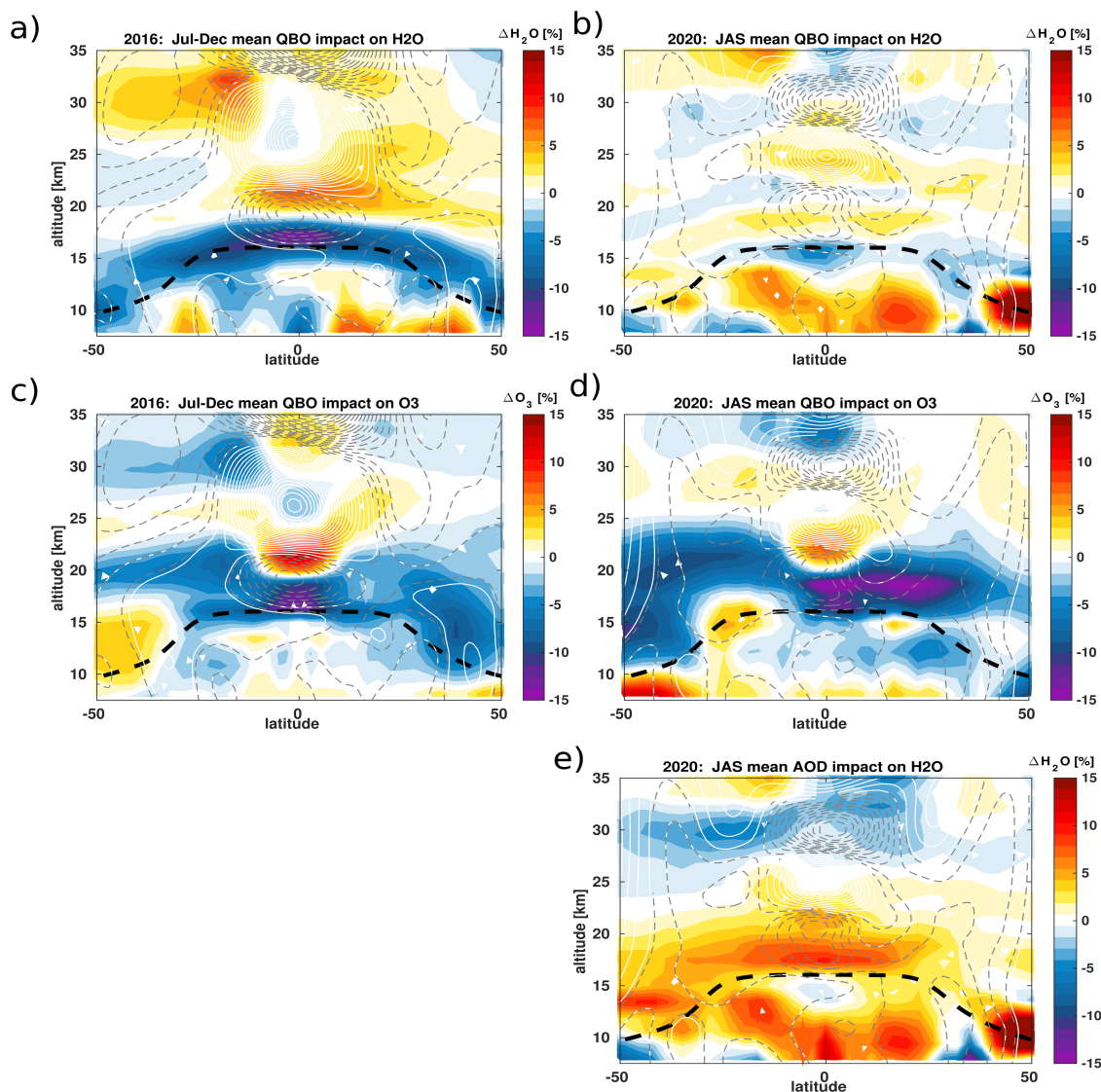


Figure 3. Zonal mean impact of the QBO disruption on the lower stratospheric H₂O (a, b) and O₃ (c, d) anomalies from MLS satellite observations averaged from July to December for 2016 (a, c) and from July to September for 2020 (b, d) period. In addition, the impact of the 2020 Australian wildfires is shown (e). All panels show the percentage change relative to monthly mean mixing ratios as a function of latitude and altitude. The impact of the QBO disruptions and the Australian wildfire on the stratospheric trace gases is derived from the multiple regression fit as the difference between the residual (ϵ in Eq. 1) without and with explicit inclusion of the QBO signal. The black dashed horizontal line indicates the tropopause from ERA5. Monthly averaged zonal mean zonal wind component, u (m s^{-1}), from ERA5, is overlaid as solid white (westerly wind) and dashed gray (easterly wind) contours lines.



tropical QBO easterly in 2020 led to a small decrease in lower stratospheric H₂O mixing ratios, therefore, to small negative lower stratospheric H₂O anomalies (Fig. 3b). Despite the similar zonal mean structure of O₃ anomalies induced by both QBO disruption events within these different averaging periods for 2016 (July–to–December) and 2020 (JAS), the impact of the QBO disruption on zonal mean O₃ mixing ratios are weaker when averaged in the entire year 2020 than in the year 2016 (Fig. 3c, d and Fig. S2c, d in the supplement). The differences in the strength and depth between the 2016 and 2020 H₂O and O₃ anomalies and their modulation by the QBO disruption events clearly suggest substantial differences in the anomalous tropical upwelling of the BDC and the tropical cold point temperatures. The smaller negative tropical O₃ anomalies suggest that the tropical upwelling of the BDC and its modulation by the QBO–induced secondary circulation are weaker in 2020 than in 2016. Simultaneously, the positive tropical H₂O anomalies in 2020 that are not related to the QBO disruption (Fig. S2b) indicate a warmer tropical cold point temperature potentially induced by the unusually strong Australian wildfire smoke in the stratosphere (Khaykin et al., 2020; Yu et al., 2021; Peterson et al., 2021). The main dynamical causes of these differences are investigated in the following section.

4.2 Mechanisms driving the strength and depth differences

To further investigate and understand the key drivers of the anomalous circulation differences between the 2015–2016 and 2019–2020 QBO disruption events, we analyse the differences in the tropical upwelling of the BDC and the secondary circulation induced by the QBO wind shear. Figure 4a–d show time series of the tropical residual circulation vertical velocity and temperature anomalies together with the impacts of the two QBO disruption events on $\overline{w^*}$ and temperature anomalies during the 2015–2016 and 2019–2020 periods, respectively. Also, latitude–altitude sections of the $\overline{w^*}$ and temperatures together with the associated impacts of the QBO disruption events during the 2015–2016 and 2019–2020 periods are shown in the supplement Fig. S4.

Clearly, there are substantial differences in the anomalous tropical upwelling of the BDC as shown by the $\overline{w^*}$ and temperatures during the two disruption events, consistent with the O₃ anomalies (Fig. 1c). Also, the modulation of the tropical upwelling by the QBO exhibits differences but smaller than anomalous circulation differences, consistent with the QBO disruption–induced O₃ anomalies (Fig. 2b). In 2016, the tropical upwelling anomalies strongly increases up to about 45 % below the altitude of about 20 km from April to December when the QBO westerly phase shifts to QBO easterly phase (Fig. 4a). However in 2020, the tropical upwelling anomalies are weaker and only reach up to about 20 % below the altitude of about 20 km, leading to about 25 % weaker $\overline{w^*}$ anomalies in 2020 than in 2016 between the altitude of about 17 km and 20 km. Below the altitude of about 17 km, the $\overline{w^*}$ anomalies are about 10 % weaker in 2020 than in 2016. In addition to the weaker tropical upwelling in 2020, the impact of the QBO disruption events on $\overline{w^*}$ anomalies is consistent with the weaker QBO–induced secondary circulation in 2020 than in 2016 with up to about 25 % weaker modulation of the tropical upwelling (Fig. 4b). This weaker tropical upwelling of the BDC and the QBO–induced secondary circulation in 2020 than in 2016 is also visible in the zonal mean cross section of the mean $\overline{w^*}$ and temperature anomalies (Fig S4a, b, e, f in the supplement), together with the impacts of the QBO disruption events on $\overline{w^*}$ and temperature anomalies for 2016 and 2020 (Fig. S4c, d, g, h in the supplement). The increase of the tropical upwelling as well as the secondary circulation induced by the QBO easterly wind shear are weaker

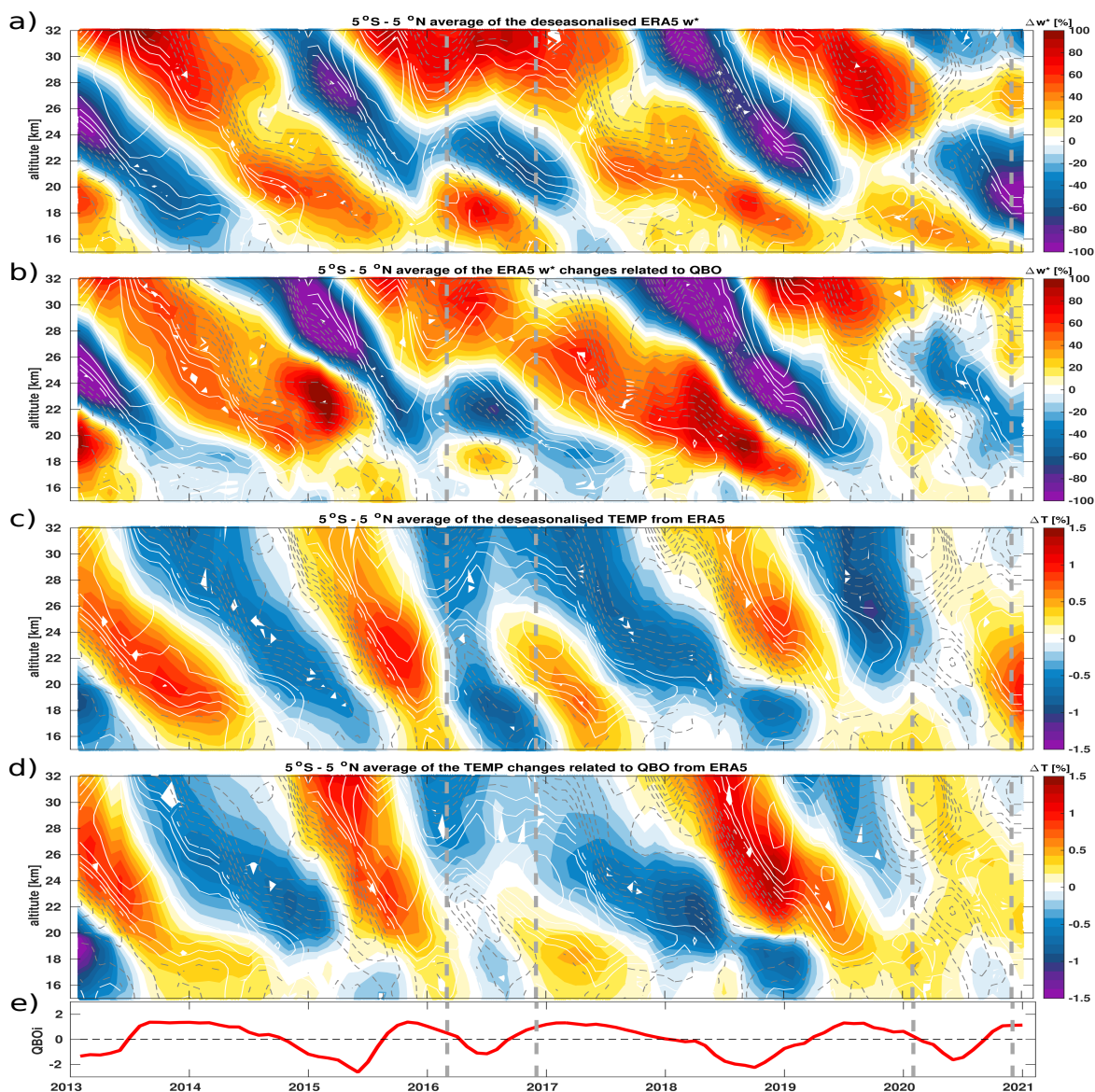


Figure 4. Tropical averaged of the deseasonalized mean residual vertical velocity ($\overline{w^*}$) (a) and temperature anomalies (b) time series from ERA5 for the 2013–2020 period together with the impact of QBO disruptions on the tropical mean $\overline{w^*}$ (c) and temperature anomalies (d) derived from the multiple regression fit as a function of latitude and altitude. (a) Deseasonalized monthly mean tropical upwelling. (b) Disrupted QBO impact on monthly mean tropical upwelling anomalies. (c) Deseasonalized monthly mean tropical temperature. (d) Disrupted QBO impact on monthly mean tropical temperature anomalies. Vertical grey dashed lines indicate the QBO disruption onset and offset years. The lowermost panel (e) shows the QBO index at 50 hPa in red. Monthly averaged zonal mean zonal wind component, u (m s^{-1}), from ERA5, is overlaid as solid white (westerly) and dashed gray (easterly) contours lines.



and shallower in 2020 than in 2016 (Fig. 4a, b and Fig. S4a–d in the supplement). The differences in the anomalous tropical upwelling and secondary circulation are also consistent with the differences in the temperature anomalies as well as in the QBO disruption–induced temperature anomalies (Fig. 4c, d and Fig. S4e–h in the supplement). In 2016, the tropical cold point temperature anomalies (at altitudes of about 17–18 km) are substantially negative (Fig. 4c in the supplement). This decrease
265 in tropical temperatures is consistent with the strong tropical upwelling of the BDC and its modulation by the QBO–induced secondary circulation, which, in turn led to large negative tropical lower stratosphere H₂O and O₃ anomalies in 2016 (Fig. 4 and Fig. S4a, c, e, g in the supplement).

Conversely, the tropical cold point temperature anomalies are warmer and barely exceeding -0.1 K in 2020, consistent with the smaller tropical $\overline{w^*}$ anomalies (Fig. 4 and Fig. S4b, d, f, h in the supplement) and the shorter lifetime of tropical O₃
270 anomalies, which last for only about 3 months (Fig. 1 and Fig. 2). These warmer tropical cold point temperature anomalies corroborate the weaker tropical upwelling of the BDC and smaller tropical lower stratospheric H₂O and O₃ mixing ratios in the year 2020. Interestingly, the differences in the tropical cold point temperature anomalies between the years 2016 and 2020 are more pronounced as shown in Figure S4e, f in the supplement than the differences in the QBO disruption–induced tropical cold point temperature anomalies (Figure S4g, h in the supplement). This anomalously warmer stratosphere, including warmer cold
275 point temperature in 2020, is consistent with recent findings about the impact of Australian wildfire smoke (Khaykin et al., 2020; Yu et al., 2021; Peterson et al., 2021). Therefore, we also pay attention to volcanic eruptions and Australian wildfire smoke in 2020, which can impact lower stratospheric temperatures, and therefore, lower stratospheric H₂O and O₃ anomalies. Indeed using our regression analyses, we can show that the Australian wildfire largely moistened the lower stratosphere between the altitude of 16 km and 25 km in 2020 by inducing anomalously warmer stratosphere, thereby, hiding the impact of 2019–
280 2020 QBO disruption on H₂O anomalies (Fig. 3e). The removal of Australian wildfire impact allows to better highlight the weak structure of the 2019–2020 disrupted QBO impact on lower stratospheric H₂O anomalies, which is similar to the 2015–2016 QBO disruption-induced effect. Regarding the difference in the upwelling of the BDC forcing, we finally investigate the related wave drag changes in the following.

To investigate the main causes of the BDC differences between the year 2016 and the year 2020 during the QBO disruption
285 events, we calculate the planetary and gravity wave drag. We analyse the differences in terms of wave activities potentially induced by specific sea surface conditions such as the unusually warm 2015–2016 El Niño and the 2019–2020 strong positive Indian Dipole Ocean, which impact tropical convective activities (Jia et al., 2014). For additional details about the wave decomposition please see Diallo et al. (2021) and Ern et al. (2014).

The BDC and its interannual variability are driven by the planetary and gravity wave breaking in different stratospheric
290 regions (Haynes et al., 1991; Rosenlof and Holton, 1993; Newman and Nash, 2000; Plumb, 2002; Shepherd, 2007). Therefore, any changes in wave drag will lead to circulation and composition changes. Figure 5a–f show the January-to-June zonal mean of the deseasonalized monthly mean net wave forcing (PWD + GWD - du/dt), planetary wave drag (PWD) and gravity wave drag (GWD) from the ERA5 reanalysis for the years 2016 and 2020, respectively. Note that the net wave forcing (NetF) is equal to the contribution of Coriolis force plus meridional advection plus vertical advection to the momentum balance (Ern et al., 2021).
295 Clearly, the net forcing anomalies as well as the planetary and gravity wave drag anomalies exhibit differences in strength and

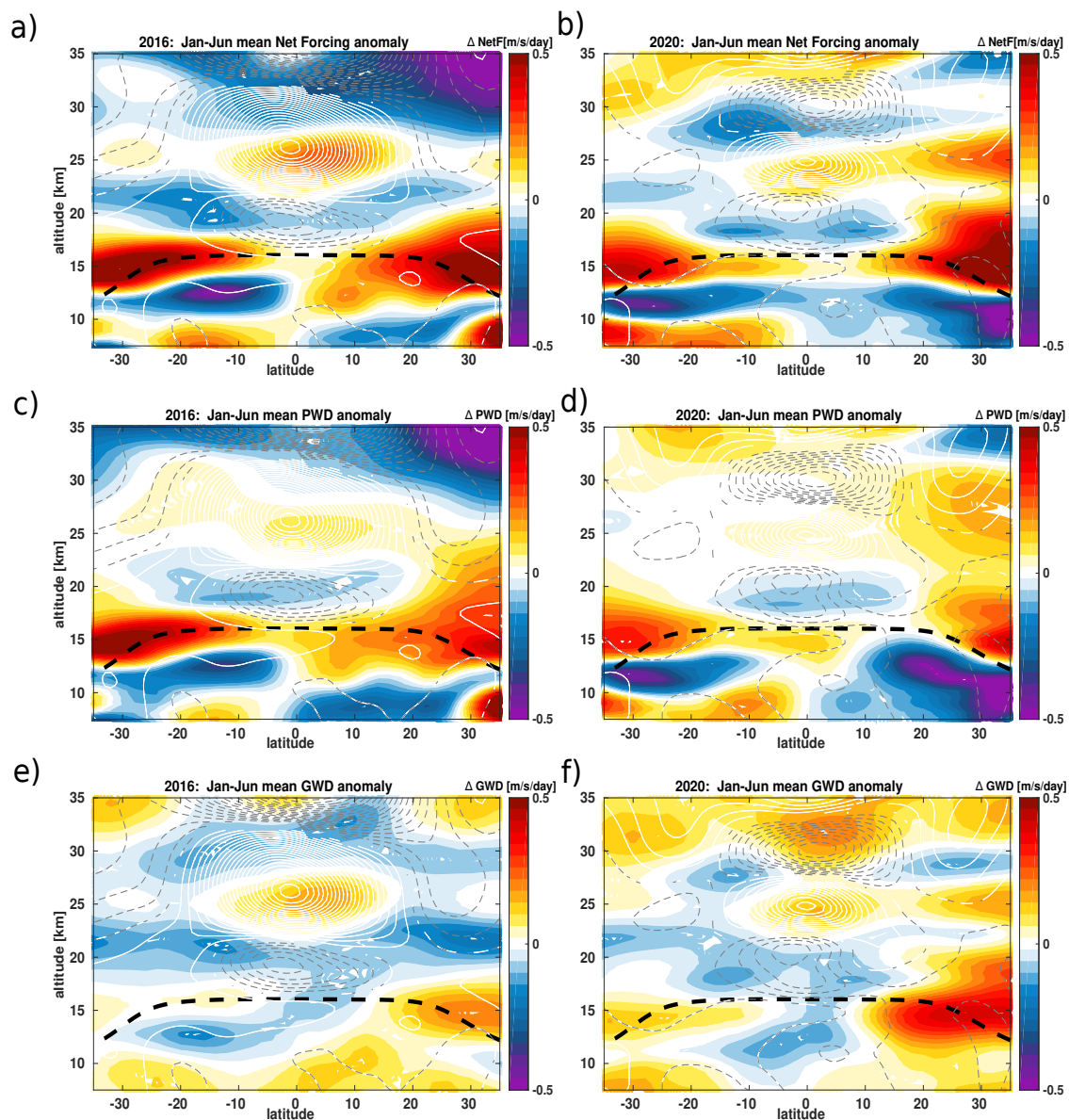


Figure 5. Deseasonalized monthly mean zonal mean net wave forcing (NetF)(a, b), planetary wave drag (PWD) (c, d) and gravity wave drag (GWD) (e, f) anomalies from the ERA5 reanalysis for the years 2016 (a, c, e) and 2020 (b, d, f) as a function of latitude and altitude. The black dashed horizontal line indicates the tropopause from ERA5. Monthly mean zonal mean wind component, u (m s^{-1}), from ERA5 is overlaid as solid gray contours (westerly) and dashed gray contours(easterly) lines.

depth in the lower stratosphere between the 2015–2016 and 2019–2020 QBO disruption events. During the 2015–2016 QBO disruption, the net wave forcing is stronger and broader in the lower stratosphere between the tropopause and the altitude of



about 25 km than during the 2019–2020 QBO disruption (Fig 5a, b). Particularly, the wave breaking near the equatorward
flanks of the subtropical jet known as a major BDC forcings region is narrower in 2020 than 2016. These differences in net
300 wave forcing are the main cause of a weaker advective BDC and its modulation by the QBO–induced secondary circulation
in 2020 than in 2016, therefore, contributing to the anomalous lower stratospheric H₂O and O₃ differences in addition to the
significant Australian wildfire effect on lower stratospheric H₂O mixing ratios. The wave forcing evolution during six months
(January–to–June) after the QBO disruptions is consistent with the zonal mean differences in wave forcings, i.e. the time series
of net forcing, planetary and gravity wave drag (Fig. S5).

305 In addition, we show the contribution of planetary (Fig 5c, d, and Fig. S5b) and gravity (Fig 5e, f and Fig. S5c) wave drag to
better understand the role of each forcing in the anomalous circulation differences during both QBO disruption events. Beside
the good agreement in the structure of planetary and gravity wave breaking, our analyses also show differences between the
2015–2016 and 2019–2020 disruption events in wave drag. The planetary and gravity wave drag indicates stronger anomalies
in wave dissipation in the lower stratosphere between the tropopause and the altitude of about 25 km during the 2015–2016
310 QBO disruption than during the 2019–2020 QBO disruption (Fig. 5c–f and Fig. S5b, c in the supplement). The anomalies in
planetary wave dissipation associated with the 2015–2016 QBO disruption are stronger and extend from the tropics toward the
subtropical jet between the tropopause and the altitude of about 25 km, while for the 2019–2020 disruption, these anomalies
are smaller and confined to the tropics. These differences in the strength and depth of the anomalies are even larger in the
gravity wave drag. During the 2015–2016 QBO disruption, gravity waves break in the entire lower stratosphere between the
315 tropopause and the altitude of about 25 km with a maximum occurring near the upper flank of the subtropical jet, a key region
for strengthening the shallow branch of the BDC (Shepherd and McLandress, 2011; Diallo et al., 2019, 2021) (Fig. 5e, f). The
differences in the strength and depth of planetary and gravity wave breaking are clearly the main cause of observed differences
in the anomalous upwelling strength of the BDC between the 2015–2016 and 2019–2020 QBO disruptions. This main cause is
a combination of planetary wave dissipation in the tropics and particularly strong gravity wave breaking near the equatorward
320 flanks of the subtropical jet during the 2015–2016 QBO disruption as shown in the previous studies (Kang et al., 2020; Kang
and Chun, 2021; Osprey et al., 2016). In summary, the strong planetary waves and gravity waves, which are likely related to
ENSO and IOD, are responsible for the tropical upwelling of the BDC differences and its modulation by the QBO–induced
secondary circulation, therefore, the negative lower stratospheric H₂O and O₃ anomalies. Regardless of the net wave forcing
in 2020, Australian wildfire led to less lower stratospheric dehydration due to the warmer stratosphere.

325 Note that during the 2015–2016 and 2019–2020 QBO disruptions, the surface conditions were different in terms of natural
variability–induced convective activity. To trace back and link the potential source of convectively generated wave activities
to regional differences, we finally analysed the monthly mean Outgoing Longwave Radiation (OLR) (Fig. 6 and Fig. S6 in
the supplement). Clearly, there are regional differences in the occurrence of strong convective events between the 2015–2016
and 2019–2020 QBO disruptions. During the 2015–2016 QBO disruption, the tropical mean OLR anomalies reveal two active
330 convective regions, namely the East Indian Ocean associated with the negative IOD in 2016, and the Central Pacific Ocean
associated with the 2015–2016 El Niño. However, during the 2019–2020 QBO disruption, the tropical mean OLR anomalies
show only one strong active convective region that is the West Indian Ocean and East Africa associated with the strong 2019

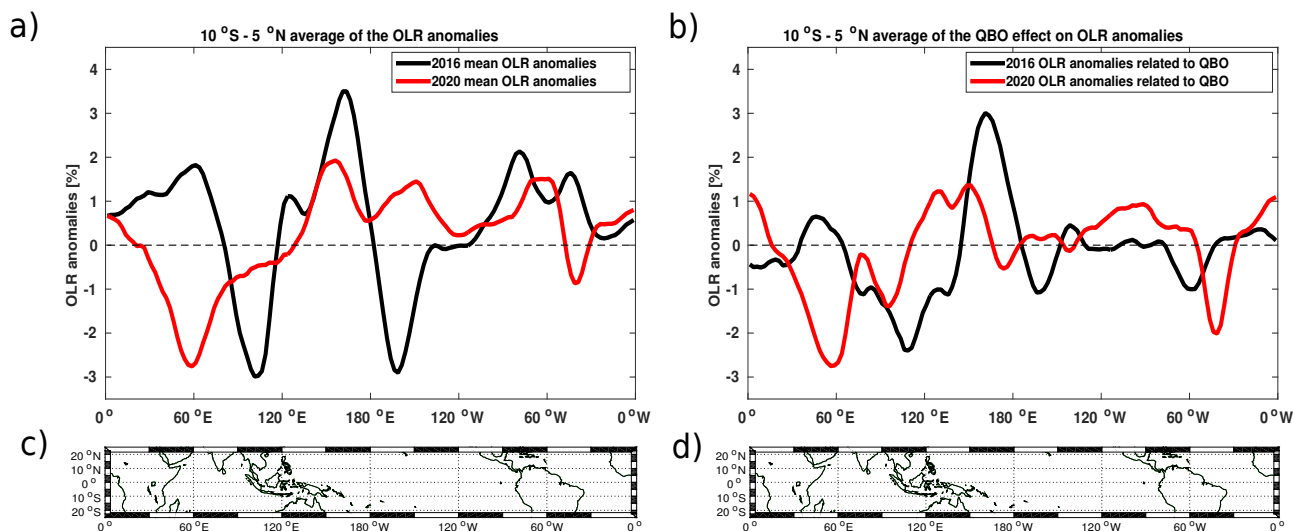


Figure 6. Longitudinal variations of the monthly mean Outgoing Longwave Radiation (OLR) anomalies (a) averaged between 20°S – 20°S together with the 2016 and 2020 QBO effect (b) associated with the convective activity derived from the multiple regression fit. The lower-most panels (c, d) shows the tropical region where the OLR timeseries are averaged.

IOD. Both QBO disruption effects related to OLR variations are linked to strong convective activity in the Indian Ocean, therefore, suggesting the importance role of this region may play in strong wave activities. This additional information related to the strength of convective activities in the Indian Ocean is of great interest for better understanding and relating the origin of the QBO disruption events and their strength based on regional forcings. This regional forcing and interplay of different modes of climate variability will be presented in further studies.

5 Summary and conclusions

Based on an established multiple regression method applied to Aura MLS observations, we found that both the 2015–2016 and 2019–2020 QBO disruptions induced similar structural changes in the lower stratospheric H_2O and O_3 anomalies. Both QBO disruptions induced negative anomalies in H_2O and O_3 , few months after the sudden shift from the QBO westerly to QBO easterly wind shear reached the tropical tropopause. During the boreal winter of 2015–2016 (September 2015–March 2016), the alignment of the strong El Niño with the QBO westerly strongly moistened the lower stratosphere between the tropopause and the altitude of 25 km (positive anomalies of more than 20%). Analogously, the alignment of the weak El Niño with the strong QBO westerly and the impact of Australian wildfire smoke strongly moistened the lower stratosphere (positive anomalies of more than 20%) during the boreal winter of 2019–2020 (September 2019–Jun 2020). The sudden shift from the QBO westerly to QBO easterly wind shear reversed the lower stratospheric moistening between the tropopause and an altitude of about 20 km , therefore leading to large negative H_2O and O_3 anomalies by the end of summer 2016 and to small negative



H₂O and moderate negative O₃ anomalies in 2020. These decreases in H₂O and O₃ mixing ratios are due to a strengthening of
350 the tropical upwelling of the BDC and cooling tropical cold point temperatures as well as their modulations by the secondary
circulation induced by the QBO wind shear, consistent with the residual vertical velocity and temperature anomalies.

However, differences occur in the strength and depth of the QBO disruption-induced negative H₂O and O₃ anomalies in the
lower stratosphere between 2016 and 2020. We found that the impact of the 2019–2020 QBO disruption on lower stratospheric
H₂O and O₃ anomalies is smaller and shallower than the 2015–2016 disrupted QBO impact. The differences in the strength
355 and depth of the O₃ anomalies and its modulation by the QBO disruption events are due to discrepancies in the anomalous
tropical upwelling of the BDC, which was up to about 25 % larger in 2016 than in 2020. The analysis of the wave drag
shows that the differences in planetary wave breaking in the tropical lower stratosphere and the gravity wave breaking near the
equatorward upper flank of the subtropical jet are the main reasons of the differences in the anomalous tropical upwelling of
the BDC and secondary circulation between the year 2016 and the year 2020. The main differences in lower stratospheric H₂O
360 anomalies between the year 2016 and the year 2020 are due to discrepancies in the tropical cold point temperatures. Despite of
the anomalous planetary waves and gravity wave activities, which are likely related to ENSO and IOD, the 2020 Australian
wildfire predominantly warmed the cold point temperature, therefore, leading to less dehydration of the lower stratosphere.

Finally, our results suggest that the interplay of QBO phases with a combination of ENSO and IOD events, and in particular
also wildfires and volcanic eruptions, will be crucial for the control of the lower stratospheric H₂O and O₃ budget in a changing
365 future climate. Especially, when increasing future warming will lead to trends in ENSO (Timmermann et al., 1999; Cai et al.,
2014) and IOD (Ihara et al., 2008) as projected by climate models, and a related potential increase in wildfire frequency
combined with a decreasing lower stratospheric QBO amplitude (Kawatani and Hamilton, 2013) are expected in future climate
projections. The interplay will change with strong El Niño/negative IOD and La Niña/strong positive IOD likely controlling
the lower stratospheric trace gas distributions and variability more strongly in a future changing climate. Clearly, both ENSO
370 and IOD impact on the tropopause height and tropical cold point temperature. Further analysis is needed using climate model
sensitivity simulations to pinpoint the impact of these future changes in lower stratospheric trace gases and the related radiative
feedback.

Data availability. MLS water vapor and ozone data were obtained from the Goddard Earth Sciences Data and Information Services Center
at es Center at doi.10.5067/Aura/MLS/DATA2508 and doi.10.5067/Aura/MLS/DATA2516, respectively. The aerosol optical depth data is
375 available through Khaykin et al. 2020. The ERA5 reanalysis are available at <https://apps.ecmwf.int/data-catalogues/era5/?class=ea>, last
access: 2nd February 2022, through Hersbach et al., 2020.

Author contributions. MD designed the study, conducted research, performed the calculation and the complete analysis of the impact of the
QBO disruptions as well as drafted the first manuscript. ME calculated the wave decomposition. FP, MH, ME, JU, SK and MR provided
helpful discussions and comments. MD edited the final draft with contributions from all co-authors for communication with the journal.



380 *Competing interests.* The authors declare that they have no conflict of interest.

Acknowledgements. Mohamadou Diallo research position is funded by the Deutsche Forschungsgemeinschaft (DFG) individual research grant number DI2618/1-1 and Institute of Energy and Climate Research, Stratosphere (IEK-7), Forschungszentrum in Jülich during which this work had been carried out. FP is funded by the Helmholtz Association under grant number VH-NG-1128 (Helmholtz Young Investigators Group A-SPECi). Manfred Ern was supported by the German Federal Ministry of Education and Research (Bundesministerium für Bildung und Forschung, BMBF) project QUBICC, grant number 01LG1905C, as part of the Role of the Middle Atmosphere in Climate II (ROMIC-II) programme of BMBF. We gratefully acknowledge the Earth System Modelling Project (ESM) for funding this work by providing computing time on the ESM partition of the supercomputer JUWELS at the Jülich Supercomputing Centre (JSC). Moreover, we particularly thank the European Centre for Medium-Range Weather Forecasts for providing the ERA5 and ERA-Interim reanalysis data.

385



References

- 390 Abalos, M., Ploeger, F., Konopka, P., Randel, W. J., and Serrano, E.: Ozone seasonality above the tropical tropopause: reconciling the Eulerian and Lagrangian perspectives of transport processes, *Atmospheric Chemistry and Physics*, 13, 10 787–10 794, <https://doi.org/10.5194/acp-13-10787-2013>, 2013.
- Andrews, D. G., Holton, J. R., and Leovy, C. B.: *Middle Atmosphere Dynamics*, vol. 40 of *International Geophysics Series*, Academic Press, San Diego, USA, 1987.
- 395 Anstey, J. A., Banyard, T. P., Butchart, N., Coy, L., Newman, P. A., Osprey, S., and Wright, C. J.: Quasi-biennial oscillation disrupted by abnormal Southern Hemisphere stratosphere, *Geophys. Res. Lett.*, <https://doi.org/10.1002/essoar.10503358.2>, 2021a.
- Anstey, J. A., Banyard, T. P., Butchart, N., Coy, L., Newman, P. A., Osprey, S., and Wright, C. J.: Prospect of increased disruption to the QBO in a changing climate, *Geophys. Res. Lett.*, <https://doi.org/10.21203/rs.3.rs-86860/v1>, 2021b.
- Baldwin, M. P., Gray, L. J., Dunkerton, T. J., Hamilton, K., Haynes, P. H., Randel, W. J., Holton, J. R., Alexander, M. J., Hirota, I., Horinouchi,
400 T., Jones, D. B. A., Kinnnersley, J. S., Marquardt, C., Sato, K., and Takahashi, M.: The quasi-biennial oscillation, *Reviews of Geophysics*, 39, 179–229, <https://doi.org/10.1029/1999RG000073>, 2001.
- Barton, C. A. and McCormack, J. P.: Origin of the 2016 QBO Disruption and Its Relationship to Extreme El Niño Events, *Geophys. Res. Lett.*, <https://doi.org/10.1002/2017GL075576>, 2017.
- Brinkop, S., Dameris, M., Jöckel, P., Garny, H., Lossow, S., and Stiller, G.: The millennium water vapour drop in chemistry–climate model
405 simulations, *Atmospheric Chemistry and Physics*, 16, 8125–8140, <https://doi.org/10.5194/acp-16-8125-2016>, 2016.
- Butchart, N.: The Brewer-Dobson circulation, *Rev. Geophys.*, 52, 157–184, <https://doi.org/10.1002/2013RG000448>, 2014.
- Butchart, N. and Scaife, A. A.: Removal of chlorofluorocarbons by increased mass exchange between the stratosphere and troposphere in a changing climate., *Nature*, 410, 799–802, <https://doi.org/10.1038/35071047>, 2001.
- Cai, W., Borlace, S., Lengaigne, M., van Rensch, P., Collins, M., Vecchi, G., Timmermann, A., Santoso, A., McPhaden, M. J., Wu, L.,
410 England, M. H., Wang, G., Guilyardi, E., and Jin, F.-F.: Increasing frequency of extreme El Niño events due to greenhouse warming, *Nat. Clim. Change*, 4, 111–116, <https://doi.org/10.1038/nclimate2100>, 2014.
- Christiansen, B., Yang, S., and Madsen, M. S.: Do strong warm ENSO events control the phase of the stratospheric QBO?, *Geophys. Res. Lett.*, 43, 10,489–10,495, <https://doi.org/10.1002/2016GL070751>, 2016.
- Coy, L., Newman, P. A., Pawson, S., and Lait, L. R.: Dynamics of the Disrupted 2015/16 Quasi-Biennial Oscillation, *J. Clim.*, 30, 5661–5674,
415 <https://doi.org/10.1175/JCLI-D-16-0663.1>, 2017.
- DallaSanta, K., Orbe, C., Rind, D., Nazarenko, L., and Jonas, J.: Response of the Quasi-Biennial Oscillation to Historical Volcanic Eruptions, *Geophysical Research Letters*, 48, e2021GL095412, <https://doi.org/https://doi.org/10.1029/2021GL095412>, e2021GL095412
2021GL095412, 2021.
- Damadeo, R. P., Zawodny, J. M., and Thomason, L. W.: Reevaluation of stratospheric ozone trends from SAGE II data using a simultaneous
420 temporal and spatial analysis, *Atmos. Chem. Phys.*, 14, 13 455–13 470, <https://doi.org/10.5194/acp-14-13455-2014>, 2014.
- Dessler, A. E., Schoeberl, M. R., Wang, T., Davis, S. M., and Rosenlof, K. H.: Stratospheric water vapor feedback, *Proceed. Nat. Acad. Sci.*, 110 45, 18 087–91, 2013.
- Diallo, M., Ploeger, F., Konopka, P., Birner, T., Müller, R., Riese, M., Garny, H., Legras, B., Ray, E., Berthet, G., and Jegou, F.: Significant
425 Contributions of Volcanic Aerosols to Decadal Changes in the Stratospheric Circulation, *Geophysical Research Letters*, 44, 10,780–10,791, <https://doi.org/10.1002/2017GL074662>, 2017.



- Diallo, M., Riese, M., Birner, T., Konopka, P., Müller, R., Hegglin, M. I., Santee, M. L., Baldwin, M., Legras, B., and Ploeger, F.: Response of stratospheric water vapor and ozone to the unusual timing of El Niño and the QBO disruption in 2015–2016, *Atmospheric Chemistry and Physics*, 18, 13 055–13 073, <https://doi.org/10.5194/acp-18-13055-2018>, 2018.
- 430 Diallo, M., Konopka, P., Santee, M. L., Müller, R., Tao, M., Walker, K. A., Legras, B., Riese, M., Ern, M., and Ploeger, F.: Structural changes in the shallow and transition branch of the Brewer–Dobson circulation induced by El Niño, *Atmospheric Chemistry and Physics*, 19, 425–446, <https://doi.org/10.5194/acp-19-425-2019>, 2019.
- Diallo, M., Ern, M., and Ploeger, F.: The advective Brewer–Dobson circulation in the ERA5 reanalysis: climatology, variability, and trends, *Atmospheric Chemistry and Physics*, 21, 7515–7544, <https://doi.org/10.5194/acp-21-7515-2021>, 2021.
- Dunkerton, T. J.: A Lagrangian mean theory of wave, mean-Flow interaction with applications to nonacceleration and its breakdown, *Rev. of Geophys.*, 18, 387–400, <https://doi.org/10.1029/RG018i002p00387>, 1980.
- 435 Dunkerton, T. J.: The quasi-biennial oscillation of 2015–2016: Hiccup or death spiral?, *Geophys. Res. Lett.*, 43, 10,547–10,552, <https://doi.org/10.1002/2016GL070921>, 2016.
- Ern, M., Ploeger, F., Preusse, P., Gille, J. C., Gray, L. J., Kalisch, S., Mlynczak, M. G., Russell, J. M., and Riese, M.: Interaction of gravity waves with the QBO: A satellite perspective, *J. Geophys. Res.: Atmospheres*, 119, 2329–2355, <https://doi.org/10.1002/2013JD020731>,
440 2014.
- Ern, M., Diallo, M., Preusse, P., Mlynczak, M. G., Schwartz, M. J., Wu, Q., and Riese, M.: The semiannual oscillation (SAO) in the tropical middle atmosphere and its gravity wave driving in reanalyses and satellite observations, *Atmos. Chem. Phys.*, 21, 13 763–13 795, <https://doi.org/10.5194/acp-21-13763-2021>, 2021.
- Forster, P. M. and Shine, K. P.: Stratospheric water vapour changes as a possible contributor to observed stratospheric cooling, *Geophys. Res. Lett.*, 26, 3309–3312, <https://doi.org/10.1029/1999GL010487>, 1999.
- 445 Forster, P. M. and Shine, K. P.: Assessing the climate impact of trends in stratospheric water vapor, *Geophys. Res. Lett.*, 29, <https://doi.org/10.1029/2001GL013909>, 2002.
- Friston, K., Ashburner, J., Kiebel, S. J., Nichols, T. E., and Penny, W. D., eds.: *Statistical Parametric Mapping: The Analysis of Functional Brain Images*, Academic Press, <http://store.elsevier.com/product.jsp?isbn=9780123725608>, 2007.
- 450 Fueglistaler, S., Dessler, A. E., Dunkerton, T. J., Folkins, I., Fu, Q., and Mote, P. W.: Tropical Tropopause Layer, *Rev. Geophys.*, 47, G1004+, <https://doi.org/10.1029/2008RG000267>, 2009.
- Fujiwara, M., Suzuki, J., Gettelman, A., Hegglin, M. I., Akiyoshi, H., and Shibata, K.: Wave activity in the tropical tropopause layer in seven reanalysis and four chemistry climate model data sets, *J. Geophys. Res. Atmos.*, 117, <https://doi.org/https://doi.org/10.1029/2011JD016808>, 2012.
- 455 Garfinkel, C. I., Hurwitz, M. M., Oman, L. D., and Waugh, D. W.: Contrasting Effects of Central Pacific and Eastern Pacific El Niño on stratospheric water vapor, *Geophys. Res. Lett.*, 40, 4115–4120, <https://doi.org/10.1002/grl.50677>, 2013.
- Geller, M. A., Zhou, X., and Zhang, M.: Simulations of the Interannual Variability of Stratospheric Water Vapor, *J. Atmos. Sci.*, 59, 1076–1085, [https://doi.org/10.1175/1520-0469\(2002\)059<1076:SOTIVO>2.0.CO;2](https://doi.org/10.1175/1520-0469(2002)059<1076:SOTIVO>2.0.CO;2), 2002.
- Gettelman, A., Hoor, P., Pan, L. L., Randel, W. J., Hegglin, M. I., and Birner, T.: The extratropical upper troposphere and lower stratosphere, *Rev. Geophys.*, 49, RG3003, <https://doi.org/10.1029/2011RG000355>, 2011.
- 460 Grimshaw, R.: Wave Action and Wave–Mean Flow Interaction, with Application to Stratified Shear Flows, *Annual Rev. of Fluid Mech.*, 16, 11–44, <https://doi.org/10.1146/annurev.fl.16.010184.000303>, 1984.



- Hartmann, D. L., Holton, J. R., and Fu, Q.: The heat balance of the tropical tropopause, cirrus, and stratospheric dehydration, *Geophys. Res. Lett.*, 28, 1969–1972, <https://doi.org/10.1029/2000GL012833>, 2001.
- 465 Haynes, P. H. and Shuckburgh, E.: Effective diffusivity as a diagnostic of atmospheric transport 2. Troposphere and lower stratosphere, *J. Geophys. Res.*, 105, 22 795–22 810, <https://doi.org/10.1029/2000JD900092>, 2000.
- Haynes, P. H., McIntyre, M. E., Shepherd, T. G., Marks, C. J., and Shine, K. P.: On the “Downward Control” of Extratropical Diabatic Circulations by Eddy-Induced Mean Zonal Forces, *J. Atmos. Sci.*, 48, 651–678, [https://doi.org/10.1175/1520-0469\(1991\)048<0651:OTCOED>2.0.CO;2](https://doi.org/10.1175/1520-0469(1991)048<0651:OTCOED>2.0.CO;2), 1991.
- 470 Hegglin, M. I., Tegtmeier, S., Anderson, J., Froidevaux, L., Fuller, R., Funke, B., Jones, A., Lingenfeller, G., Lumpe, J., Pendlebury, D., Remsberg, E., Rozanov, A., Toohey, M., Urban, J., Clarmann, T., Walker, K. A., Wang, R., and Weigel, K.: SPARC Data Initiative: Comparison of water vapor climatologies from international satellite limb sounders, *J. Geophys. Res.: Atmospheres*, 118, 11,824–11,846, <https://doi.org/10.1002/jgrd.50752>, 2013.
- Hegglin, M. I., Tegtmeier, S., Anderson, J., Bourassa, A. E., Brohede, S., Degenstein, D., Froidevaux, L., Funke, B., Gille, J., Kasai, Y.,
475 Kyrölä, E. T., Lumpe, J., Murtagh, D., Neu, J. L., Pérot, K., Remsberg, E. E., Rozanov, A., Toohey, M., Urban, J., von Clarmann, T., Walker, K. A., Wang, H.-J., Arosio, C., Damadeo, R., Fuller, R. A., Lingenfeller, G., McLinden, C., Pendlebury, D., Roth, C., Ryan, N. J., Sioris, C., Smith, L., and Weigel, K.: Overview and update of the SPARC Data Initiative: comparison of stratospheric composition measurements from satellite limb sounders, *Earth Syst. Sci. Data*, 13, 1855–1903, <https://doi.org/10.5194/essd-13-1855-2021>, 2021.
- Hersbach, H., Bell, B., Berrisford, P., Hirahara, S., Horányi, A., Muñoz-Sabater, J., Nicolas, J., Peubey, C., Radu, R., Schepers, D., Simmons,
480 A., Soci, C., Abdalla, S., Abellan, X., Balsamo, G., Bechtold, P., Biavati, G., Bidlot, J., Bonavita, M., De Chiara, G., Dahlgren, P., Dee, D., Diamantakis, M., Dragani, R., Flemming, J., Forbes, R., Fuentes, M., Geer, A., Haimberger, L., Healy, S., Hogan, R. J., Hólm, E., Janisková, M., Keeley, S., Laloyaux, P., Lopez, P., Lupu, C., Radnoti, G., de Rosnay, P., Rozum, I., Vamborg, F., Villaume, S., and Thépaut, J.-N.: The ERA5 Global Reanalysis, *Q. J. R. Meteorol. Soc.*, n/a, <https://doi.org/10.1002/qj.3803>, 2020.
- Hitchcock, P., Haynes, P. H., Randel, W. J., and Birner, T.: The Emergence of Shallow Easterly Jets within QBO Westerlies, *J. Atmos. Sci.*,
485 75, 21–40, <https://doi.org/10.1175/JAS-D-17-0108.1>, 2018.
- Holton, J. R.: Equatorial Wave-Mean Flow Interaction: A Numerical Study of the Role of Latitudinal Shear, *J. Atmos. Sci.*, 36, 1030–1040, [https://doi.org/10.1175/1520-0469\(1979\)036<1030:EWMFIA>2.0.CO;2](https://doi.org/10.1175/1520-0469(1979)036<1030:EWMFIA>2.0.CO;2), 1979.
- Holton, J. R. and Gettelman, A.: Horizontal transport and the dehydration of the stratosphere, *Geophys. Res. Lett.*, 28, 2799–2802, <https://doi.org/10.1029/2001GL013148>, 2001.
- 490 Holton, J. R. and Tan, H.-C.: The Influence of the Equatorial Quasi-Biennial Oscillation on the Global Circulation at 50 mb, *Journal of the Atmospheric Sciences*, 37, 2200–2208, [https://doi.org/10.1175/1520-0469\(1980\)037<2200:TIOTEQ>2.0.CO;2](https://doi.org/10.1175/1520-0469(1980)037<2200:TIOTEQ>2.0.CO;2), 1980.
- Hu, D., Tian, W., Guan, Z., Guo, Y., and Dhomse, S.: Longitudinal Asymmetric Trends of Tropical Cold-Point Tropopause Temperature and Their Link to Strengthened Walker Circulation, *J. Clim.*, 29, 7755–7771, <https://doi.org/10.1175/JCLI-D-15-0851.1>, 2016.
- Iglesias-Suarez, F., Wild, O., Kinnison, D. E., Garcia, R. R., Marsh, D. R., Lamarque, J.-F., Ryan, E. M., Davis, S. M., Eichinger, R., Saiz-
495 Lopez, A., and Young, P. J.: Tropical Stratospheric Circulation and Ozone Coupled to Pacific Multi-Decadal Variability, *Geophysical Research Letters*, 48, e2020GL092 162, <https://doi.org/https://doi.org/10.1029/2020GL092162>, 2021.
- Ihara, C., Kushnir, Y., and Cane, M. A.: Warming Trend of the Indian Ocean SST and Indian Ocean Dipole from 1880 to 2004, *J. of Clim.*, 21, 2035 – 2046, <https://doi.org/10.1175/2007JCLI1945.1>, 2008.
- Jensen, E. J., Toon, O. B., Pfister, L., and Selkirk, H. B.: Dehydration of the upper troposphere and lower stratosphere by subvisible cirrus
500 clouds near the tropical tropopause, *Geophys. Res. Lett.*, 23, 825–828, <https://doi.org/10.1029/96GL00722>, 1996.



- Jia, J. Y., Preusse, P., Ern, M., Chun, H.-Y., Gille, J. C., Eckermann, S. D., and Riese, M.: Sea surface temperature as a proxy for convective gravity wave excitation: a study based on global gravity wave observations in the middle atmosphere, *Annales Geophysicae*, 32, 1373–1394, <https://doi.org/10.5194/angeo-32-1373-2014>, 2014.
- Kang, M.-J. and Chun, H.-Y.: Contributions of equatorial planetary waves and small-scale convective gravity waves to the 2019/20 QBO
505 disruption, *Atmos. Chem. Phys.*, 2021, 1–33, <https://doi.org/10.5194/acp-2021-85>, 2021.
- Kang, M.-J., Chun, H.-Y., and Garcia, R. R.: Role of equatorial waves and convective gravity waves in the 2015/16 quasi-biennial oscillation disruption, *Atmos. Chem. Phys.*, 20, 14 669–14 693, <https://doi.org/10.5194/acp-20-14669-2020>, 2020.
- Kawatani, Y. and Hamilton, K.: Weakened stratospheric quasibiennial oscillation driven by increased tropical mean upwelling, *Nature*, 497, 478–481, <https://doi.org/doi:10.1038/nature12140>, 2013.
- 510 Kawatani, Y., Hamilton, K., and Watanabe, S.: The Quasi-Biennial Oscillation in a Double CO₂ Climate, *J. Atmos. Sci.*, 68, 265–283, <https://doi.org/10.1175/2010JAS3623.1>, 2011.
- Kawatani, Y., Hamilton, K., Miyazaki, K., Fujiwara, M., and Anstey, J. A.: Representation of the tropical stratospheric zonal wind in global atmospheric reanalyses, *Atmos. Chem. Phys.*, 16, 6681–6699, <https://doi.org/10.5194/acp-16-6681-2016>, 2016.
- Khaykin, S., Legras, B., and Bucci, S. e. a.: The 2019/20 Australian wildfires generated a persistent smoke-charged vortex rising up to 35km
515 altitude, *Commun. Earth Environ.*, 1, <https://doi.org/10.1038/s43247-020-00022-5>, 2020.
- Kim, J. and Son, S.-W.: Tropical Cold-Point Tropopause: Climatology, Seasonal Cycle, and Intraseasonal Variability Derived from COSMIC GPS Radio Occultation Measurements, *J. of Clim.*, 25, 5343–5360, <https://doi.org/10.1175/JCLI-D-11-00554.1>, 2012.
- Kim, Y.-H. and Chun, H.-Y.: Momentum forcing of the quasi-biennial oscillation by equatorial waves in recent reanalyses, *Atmos. Chem. Phys.*, 15, 6577–6587, <https://doi.org/10.5194/acp-15-6577-2015>, 2015.
- 520 Kroll, C. A., Dacie, S., Azoulay, A., Schmidt, H., and Timmreck, C.: The Impact of Volcanic Eruptions of Different Magnitude on Stratospheric Water Vapour in the Tropics, *Atmos. Chem. Phys.*, 2020, 1–45, <https://doi.org/10.5194/acp-2020-1191>, 2020.
- Liess, S. and Geller, M. A.: On the relationship between QBO and distribution of tropical deep convection, *J. Geophys. Res.: Atmospheres*, 117, <https://doi.org/10.1029/2011JD016317>, 2012.
- Lin, P., Held, I., and Ming, Y.: The Early Development of the 2015/16 Quasi-Biennial Oscillation Disruption, *Journal of the Atmospheric
525 Sciences*, 76, 821 – 836, <https://doi.org/10.1175/JAS-D-18-0292.1>, 2019.
- Lindzen, R. S.: Equatorial Planetary Waves in Shear. Part I, *Journal of Atmos. Sci.*, 28, 609 – 622, [https://doi.org/10.1175/1520-0469\(1971\)028<0609:EPWISP>2.0.CO;2](https://doi.org/10.1175/1520-0469(1971)028<0609:EPWISP>2.0.CO;2), 1971.
- Livesey, N. J., Read, W. G., Wagner, P. A., Froidevaux, L., Lambert, A., Manney, G. L., Millán Valle, L. F., Pumphrey, H. C., Santee, M. L., Schwartz, M. J., Wang, S., Fuller, R. A., Jarnot, R. F., Knosp, B. W., and Martinez, E.: Aura Microwave Limb Sounder (MLS) Version 4.2x
530 Level 2 data quality and description document, Tech. Rep. JPL D-33509 Rev. C, pp. 1–169, <https://doi.org/10.5194/acp-15-9945-2015>, 2017.
- Match, A. and Fueglistaler, S.: Anomalous Dynamics of QBO Disruptions Explained by 1D Theory with External Triggering, *Journal of the Atmospheric Sciences*, 78, 373 – 383, <https://doi.org/10.1175/JAS-D-20-0172.1>, 2021.
- Newman, P. A. and Nash, E. R.: Quantifying the wave driving of the stratosphere, *J. Geophys. Res.: Atmospheres*, 105, 12 485–12 497, <https://doi.org/10.1029/1999JD901191>, 2000.
- 535 Newman, P. A., Coy, L., Pawson, S., and Lait, L. R.: The anomalous change in the QBO in 2015–2016, *Geophys. Res. Lett.*, 43, 8791–8797, <https://doi.org/10.1002/2016GL070373>, 2016.



- Niwano, M., Yamazaki, K., and Shiotani, M.: Seasonal and QBO variations of ascent rate in the tropical lower stratosphere as inferred from UARS HALOE trace gas data, *J. Geophys. Res.*, 108, 4794, <https://doi.org/10.1029/2003JD003871>, 4794, 2003.
- 540 Nowack, P., Abraham, N., Maycock, A., Braesicke, P., Gregory, J., Joshi, M., Osprey, A., and Pyle, J.: A large ozone-circulation feedback and its implications for global warming assessments, *Nature Climate Change*, 5, 41–45, <https://doi.org/10.1038/NCLIMATE2451>, 2015.
- Osprey, S. M., Butchart, N., Knight, J. R., Scaife, A. A., Hamilton, K., Anstey, J. A., Schenzinger, V., and Zhang, C.: An unexpected disruption of the atmospheric quasi-biennial oscillation, *Science*, <https://doi.org/10.1126/science.aah4156>, 2016.
- Peterson, D. A., Fromm, M. D., McRae, R. H. D., Campbell, J. R., Hyer, Edward J. Taha, G., Camacho, C. P., Kablick, G. P., Schmidt, C. C.,
545 and DeLand, M. T.: Australia’s Black Summer pyrocumulonimbus super outbreak reveals potential for increasingly extreme stratospheric smoke events, *npj Climate and Atmos. Sci.*, 4, 2397–3722, <https://doi.org/10.1038/s41612-021-00192-9>, 2021.
- Plumb, R. A.: The Interaction of Two Internal Waves with the Mean Flow: Implications for the Theory of the Quasi-Biennial Oscillation, *Journal of the Atmospheric Sciences*, 34, 1847–1858, [https://doi.org/10.1175/1520-0469\(1977\)034<1847:TIOTIW>2.0.CO;2](https://doi.org/10.1175/1520-0469(1977)034<1847:TIOTIW>2.0.CO;2), 1977.
- Plumb, R. A.: Stratospheric transport, *J. Meteor. Soc. Japan*, 80, 793–809, 2002.
- 550 Plumb, R. A. and Bell, R. C.: A model of the quasi-biennial oscillation on an equatorial beta-plane, *Quarterly Journal of the Royal Meteorological Society*, 108, 335–352, <https://doi.org/https://doi.org/10.1002/qj.49710845604>, 1982.
- Randel, W. and Park, M.: Diagnosing Observed Stratospheric Water Vapor Relationships to the Cold Point Tropical Tropopause, *J. Geophys. Res. Atmos.*, 124, 7018–7033, <https://doi.org/https://doi.org/10.1029/2019JD030648>, 2019.
- Randel, W. J. and Thompson, A. M.: Interannual variability and trends in tropical ozone derived from SAGE II satellite data and SHADOZ
555 ozonesondes, *Journal of Geophysical Research: Atmospheres*, 116, <https://doi.org/https://doi.org/10.1029/2010JD015195>, 2011.
- Randel, W. J., Wu, F., Vömel, H., Nedoluha, G. E., and Forster, P.: Decreases in stratospheric water vapor after 2001: Links to changes in the tropical tropopause and the Brewer-Dobson circulation, *J. Geophys. Res.*, 111, 12312, <https://doi.org/10.1029/2005JD006744>, d12312, 2006.
- Randel, W. J., Park, M., Wu, F., and Livesey, N.: A Large Annual Cycle in Ozone above the Tropical Tropopause Linked to the Brewer
560 Dobson Circulation, *J. Atmos. Sci.*, 64, 4479–4488, <https://doi.org/10.1175/2007JAS2409.1>, 2007.
- Ray, E. A., Portmann, R. W., Yu, P., and al.: The influence of the stratospheric Quasi-Biennial Oscillation on trace gas levels at the Earth’s surface, *Nature Geoscience*, 13, 1752–0908, <https://doi.org/10.1038/s41561-019-0507-3>, 2020.
- Renaud, A., Nadeau, L.-P., and Venaille, A.: Periodicity Disruption of a Model Quasibiennial Oscillation of Equatorial Winds, *Phys. Rev. Lett.*, 122, 214504, <https://doi.org/10.1103/PhysRevLett.122.214504>, 2019.
- 565 Riese, M., Ploeger, F., Rap, A., Vogel, B., Konopka, P., Dameris, M., and Forster, P.: Impact of uncertainties in atmospheric mixing on simulated UTLS composition and related radiative effects, *J. Geophys. Res.*, 117, D16305, <https://doi.org/10.1029/2012JD017751>, 2012.
- Rosenlof, K. and Holton, J.: Estimates of the stratospheric residual circulation using the downward control principle, *J. Geophys. Res.*, 98, 10465–10479, 1993.
- Saji, N., Goswami, B., Vinayachandran, P., and Yamagata, T.: A dipole mode in the tropical Indian Ocean, *Nature*, 401, 360–363,
570 <https://doi.org/10.1038/43854>, 1999.
- Santee, M. L., Manney, G. L., Livesey, N. J., Schwartz, M. J., Neu, J. L., and Read, W. G.: A comprehensive overview of the climatological composition of the Asian summer monsoon anticyclone based on 10 years of Aura Microwave Limb Sounder measurements, *J. Geophys. Res.: Atmospheres*, 122, 5491–5514, <https://doi.org/10.1002/2016JD026408>, 2017.
- Saravanan, R.: A Multiwave Model of the Quasi-biennial Oscillation, *J. Atmos. Sci.*, 47, 2465–2474, [https://doi.org/10.1175/1520-0469\(1990\)047<2465:AMMOTQ>2.0.CO;2](https://doi.org/10.1175/1520-0469(1990)047<2465:AMMOTQ>2.0.CO;2), 1990.
- 575



- Schirber, S.: Influence of ENSO on the QBO: Results from an ensemble of idealized simulations, *Journal of Geophysical Research: Atmospheres*, 120, 1109–1122, <https://doi.org/https://doi.org/10.1002/2014JD022460>, 2015.
- Schoeberl, M. R. and Dessler, A. E.: Dehydration of the stratosphere, *Atmos. Chem. Phys.*, 11, 8433–8446, <https://doi.org/10.5194/acp-11-8433-2011>, 2011.
- 580 Shepherd, T. G.: Transport in the Middle Atmosphere, *J. Meteorol. Soc. of Japan. Ser. II*, 85B, 165–191, <https://doi.org/10.2151/jmsj.85B.165>, 2007.
- Shepherd, T. G. and McLandress, C.: A Robust Mechanism for Strengthening of the Brewer–Dobson Circulation in Response to Climate Change: Critical-Layer Control of Subtropical Wave Breaking, *J. Atmos. Sci.*, 68, 784–797, <https://doi.org/10.1175/2010JAS3608.1>, 2011.
- Smith, J. W., Haynes, P. H., Maycock, A. C., Butchart, N., and Bushell, A. C.: Sensitivity of stratospheric water vapour to variability in tropical tropopause temperatures and large-scale transport, *Atmospheric Chemistry and Physics*, 21, 2469–2489, <https://doi.org/10.5194/acp-21-2469-2021>, 2021.
- 585 Solomon, S., Rosenlof, K. H., Portmann, R. W., Daniel, J. S. Davis, S. M., Sanford, T., and Plattner, G.-K.: Contributions of Stratospheric Water Vapor to Decadal Changes in the Rate of Global Warming, *Science*, 327, 1219–1223, <https://doi.org/10.1126/science.1182488>, 2010.
- 590 Son, S.-W., Lim, Y., Yoo, C., Hendon, H. H., and Kim, J.: Stratospheric Control of the Madden–Julian Oscillation, *Journal of Climate*, 30, 1909 – 1922, <https://doi.org/10.1175/JCLI-D-16-0620.1>, 2017.
- Stolarski, R. S., Waugh, D. W., Wang, L., Oman, L. D., Douglass, A. R., and Newman, P. A.: Seasonal variation of ozone in the tropical lower stratosphere: Southern tropics are different from northern tropics, *J. Geophys. Res. Atmos.*, 119, 6196–6206, <https://doi.org/https://doi.org/10.1002/2013JD021294>, 2014.
- 595 Taguchi, M.: Observed connection of the stratospheric quasi-biennial oscillation with El Niño–Southern Oscillation in radiosonde data, *J. Geophys. Res.: Atmospheres*, 115, <https://doi.org/10.1029/2010JD014325>, 2010.
- Tao, M., Konopka, P., Ploeger, F., Yan, X., Wright, J. S., Diallo, M., Fueglistaler, S., and Riese, M.: Multitimescale variations in modeled stratospheric water vapor derived from three modern reanalysis products, *Atmos. Chem. Phys.*, 19, 6509–6534, <https://doi.org/10.5194/acp-19-6509-2019>, 2019.
- 600 Thomason, L. W., Ernest, N., Millán, L., Rieger, L., Bourassa, A., Vernier, J.-P., Manney, G., Luo, B., Arfeuille, F., and Peter, T.: A global space-based stratospheric aerosol climatology: 1979–2016, *Earth Sys. Sci. Data*, 10, 469–492, <https://doi.org/10.5194/essd-10-469-2018>, 2018.
- Tian, E. W., Su, H., Tian, B., and Jiang, J. H.: Interannual variations of water vapor in the tropical upper troposphere and the lower and middle stratosphere and their connections to ENSO and QBO, *Atmospheric Chemistry and Physics*, 19, 9913–9926, <https://doi.org/10.5194/acp-19-9913-2019>, 2019.
- 605 Timmermann, A., Oberhuber, J., Bacher, A., Esch, M., Latif, M., and Roeckner, E.: El Niño, La Nina, and the Southern Oscillation, *Nature*, 398, 904–905, <https://doi.org/10.1038/19505>, 1999.
- Tweedy, O. V., Kramarova, N. A., Strahan, S. E., Newman, P. A., Coy, L., Randel, W. J., Park, M., Waugh, D. W., and Frith, S. M.: Response of trace gases to the disrupted 2015–2016 quasi-biennial oscillation, *Atmos. Chem. Phys.*, 17, 6813–6823, <https://doi.org/10.5194/acp-17-6813-2017>, 2017.
- 610 von Storch, H. and Zwiers, F. W.: *Statistical analysis in climate research*, Cambridge Univ. Press, 1999.
- Watanabe, S., Hamilton, K., Osprey, S., Kawatani, Y., and Nishimoto, E.: First Successful Hindcasts of the 2016 Disruption of the Stratospheric Quasi-biennial Oscillation, *Geophys. Res. Lett.*, 45, 1602–1610, <https://doi.org/https://doi.org/10.1002/2017GL076406>, 2018.



- 615 Weber, M., Dikty, S., Burrows, J. P., Garny, H., Dameris, M., Kubin, A., Abalichin, J., and Langematz, U.: The Brewer-Dobson circulation and total ozone from seasonal to decadal time scales, *Atmospheric Chemistry and Physics*, 11, 11 221–11 235, <https://doi.org/10.5194/acp-11-11221-2011>, 2011.
- WMO: Scientific Assessment of Ozone Depletion: 2018, Global ozone research and monitoring project - report no. 58, WMO (World Meteorological Organization), Geneva, 2018.
- 620 Wolter, K. and Timlin, M. S.: El Nino/Southern Oscillation behaviour since 1871 as diagnosed in an extended multivariate ENSO index (MEI.ext), *Int. J. Climatol.*, 31, 1074–1087, <https://doi.org/10.1002/joc.2336>, 2011.
- Yu, P., Davis, S. M., Toon, O. B., Portmann, R. W., Bardeen, C. G., Barnes, J. E., Telg, H., Maloney, C., and Rosenlof, K. H.: Persistent Stratospheric Warming Due to 2019-2020 Australian Wildfire Smoke, *Geophys. Res. Lett.*, 48, e2021GL092609, <https://doi.org/https://doi.org/10.1029/2021GL092609>, e2021GL092609 2021GL092609, 2021.